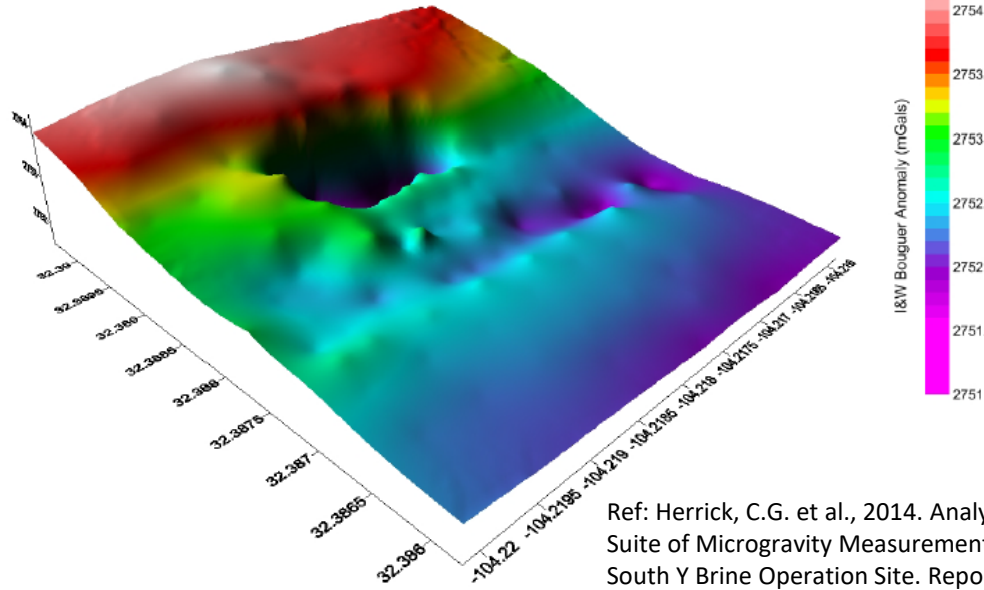


Rucker Exhibit 2 – Indications of Possible Complicating Geologic Factors



Ref: Herrick, C.G. et al., 2014. Analysis of a Comprehensive Suite of Microgravity Measurements Conducted over the South Y Brine Operation Site. Report SAND2014-0207P, January 13.

Figure 20. Plot of the Bouguer anomalies using the spherical variogram model on a 3D contour plot.

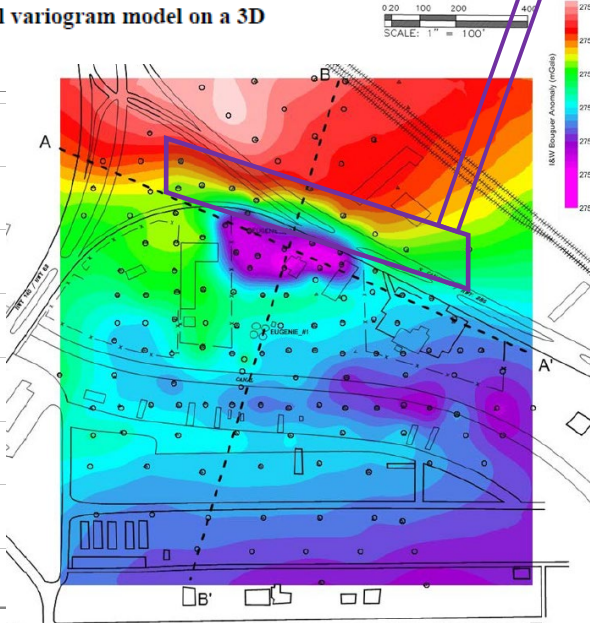
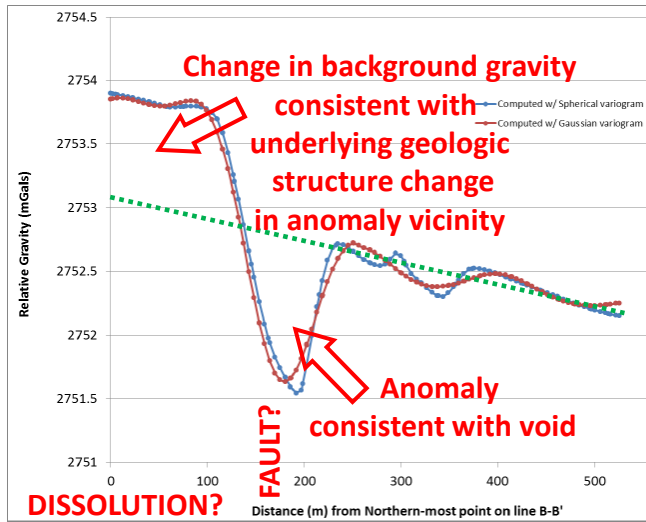
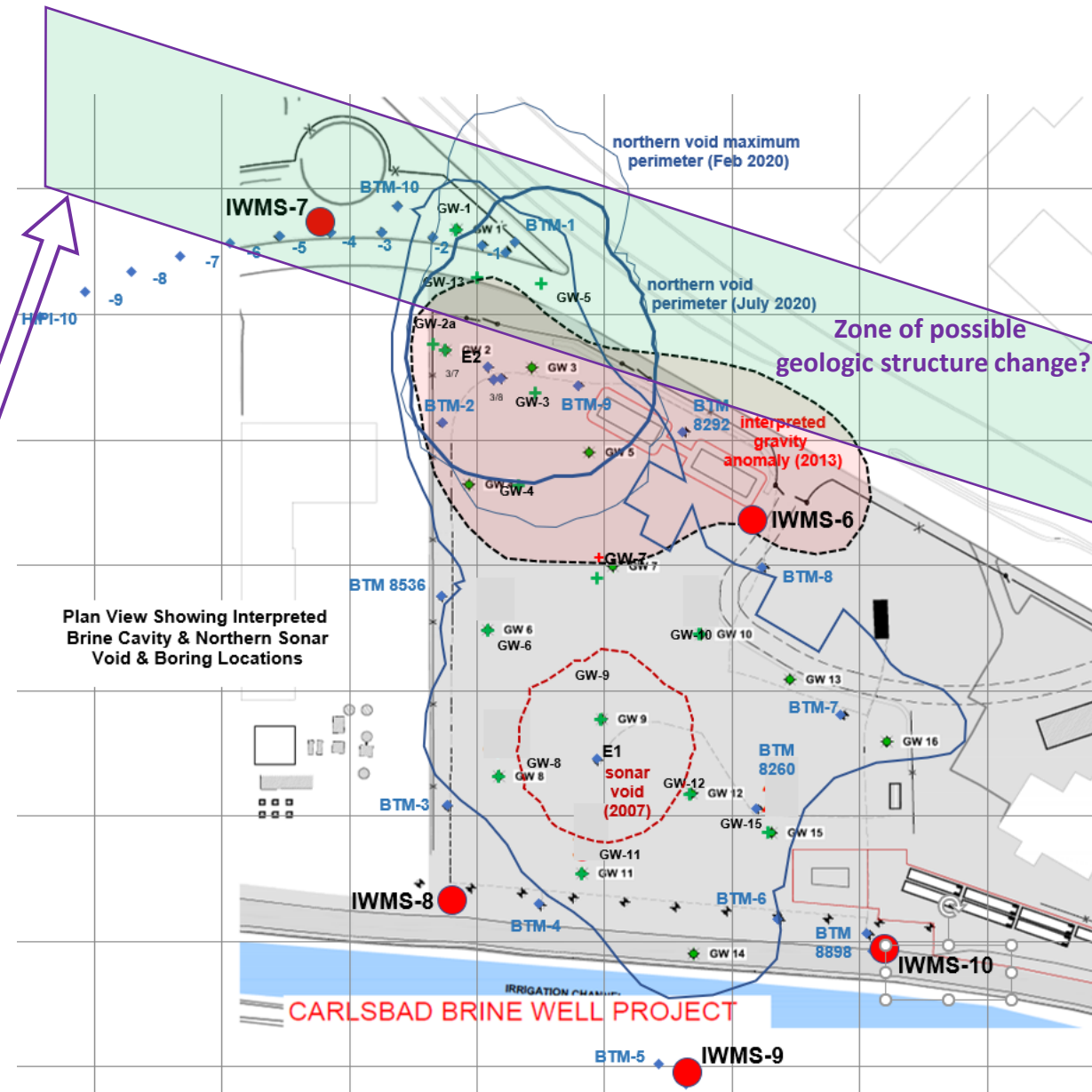


Figure 19. Contour plot of the Bouguer anomalies using the spherical variogram model.

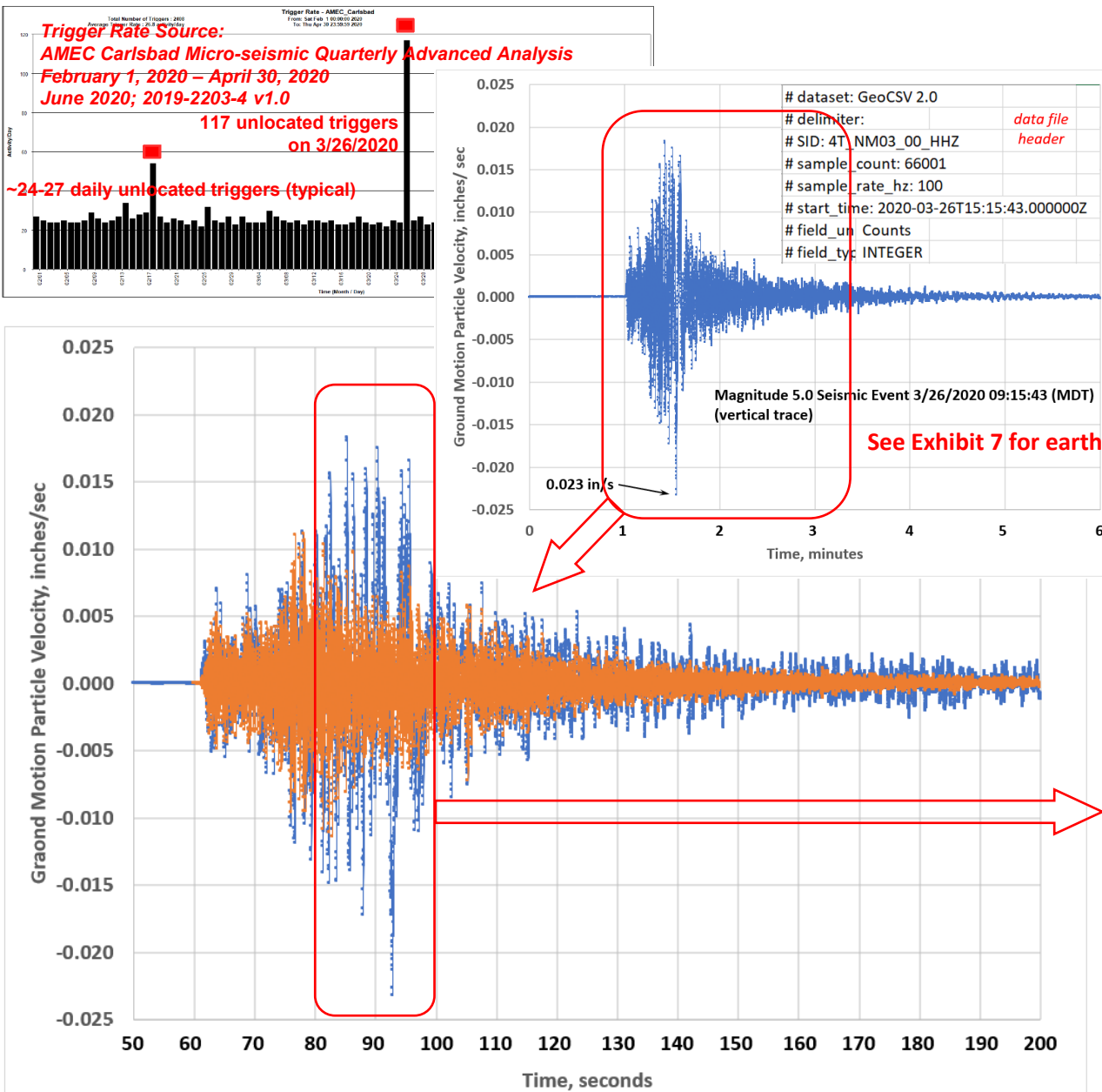


Plan View Showing Interpreted Brine Cavity & Northern Sonar Void & Boring Locations

Enhanced onsite micro-seismic network, operational in 2019

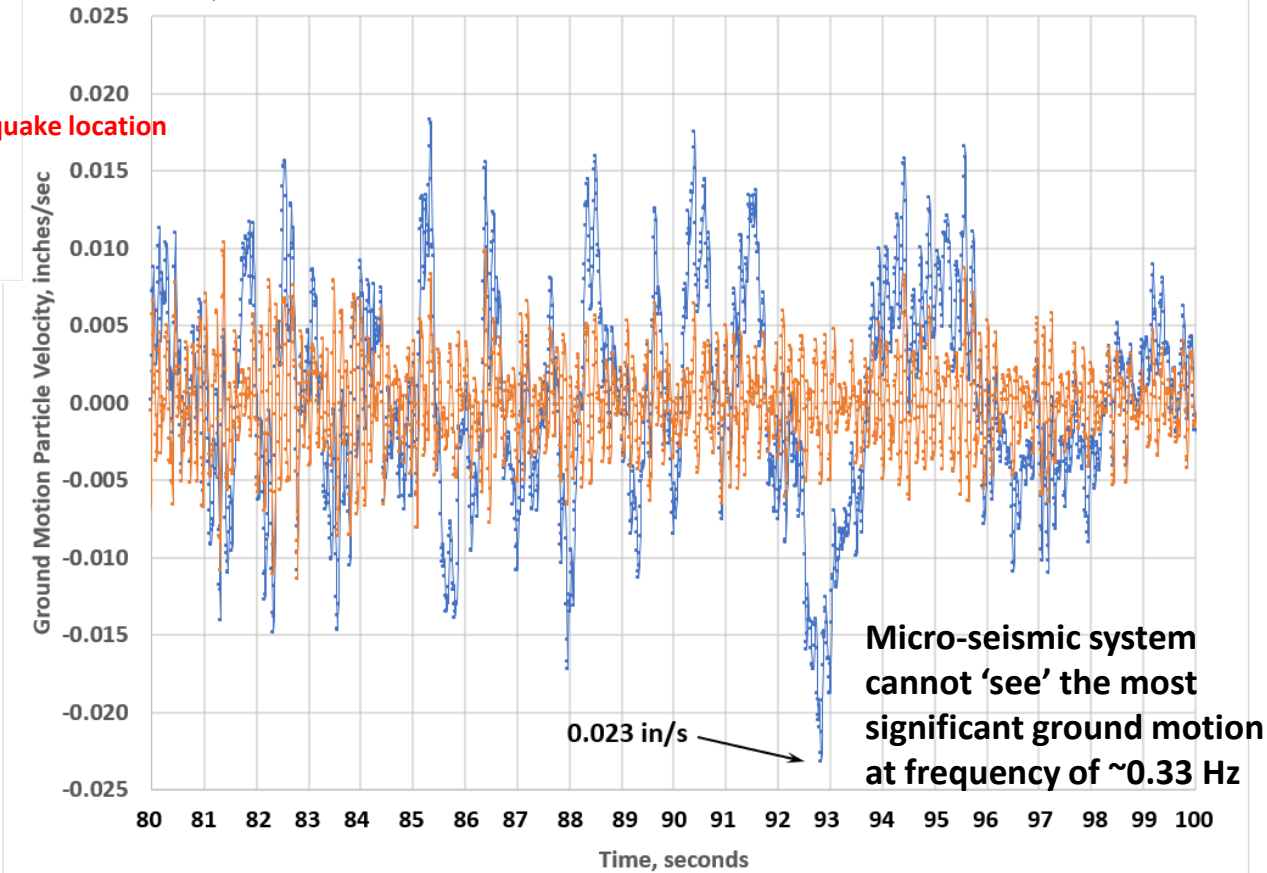
Initial offsite micro-seismic network, operational in 2014

Rucker Exhibit 3 – Conceptual Visualization: Micro-Seismic System Response to Earthquake



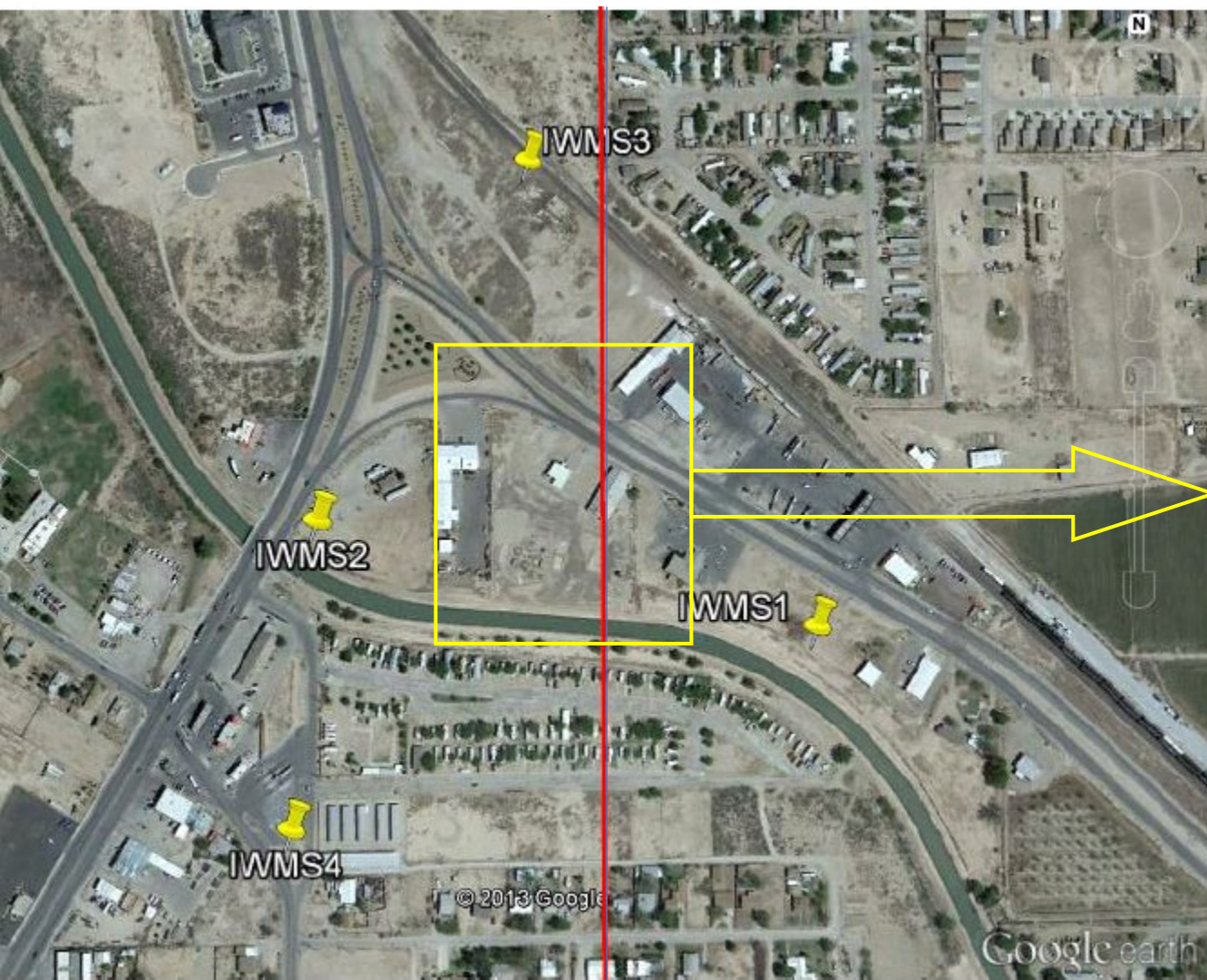
Micro-seismic system is unable to measure earthquake very low frequencies

The micro-seismic (MS) network sensors have a linear response down to 15 Hz; they are optimized to measure MS events in a range of Magnitude -2.0 to 0.0. This is the magnitude range to locate and quantify fracturing in a stressed rock formation prior to and during failure. To approximate MS sensor frequency response, the earthquake time history (sampled at 100 Hz) measured by a modern seismograph is averaged over a time period of 0.2 seconds (5 Hz) and the averaged result is subtracted from the original time history (shown in blue). This mathematically removes the low frequency portion of the time history, but retains the high frequency portion as shown in the orange trace below. The high frequency (orange) trace is consistent with what the Micro-seismic system can measure.

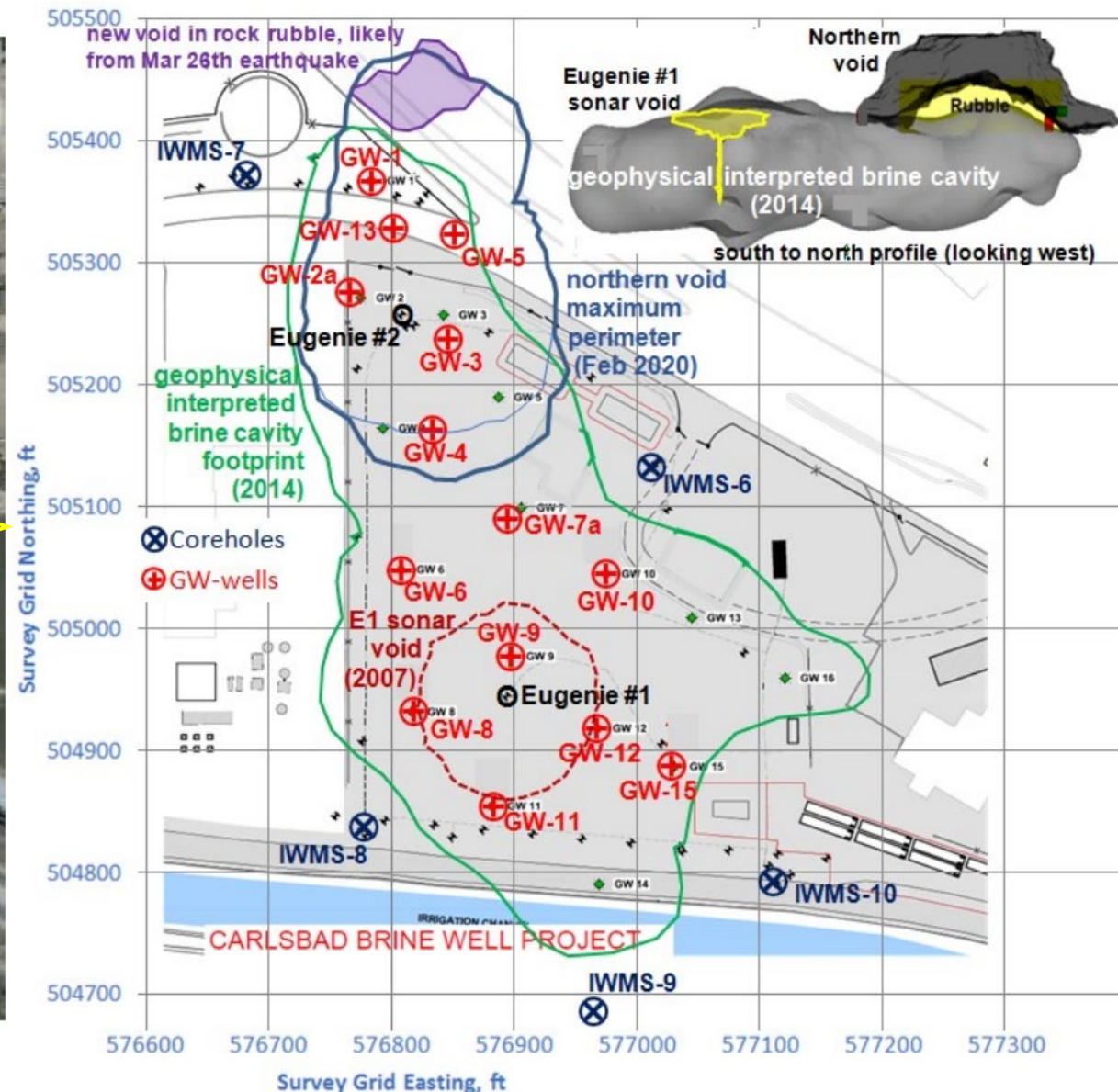


Time history is from Station T4.NM03; see Exhibit C.

Rucker Exhibit 4 – Site Layout Showing Micro-seismic Stations (IWMS-#)



Initial offsite micro-seismic network, operational in 2014

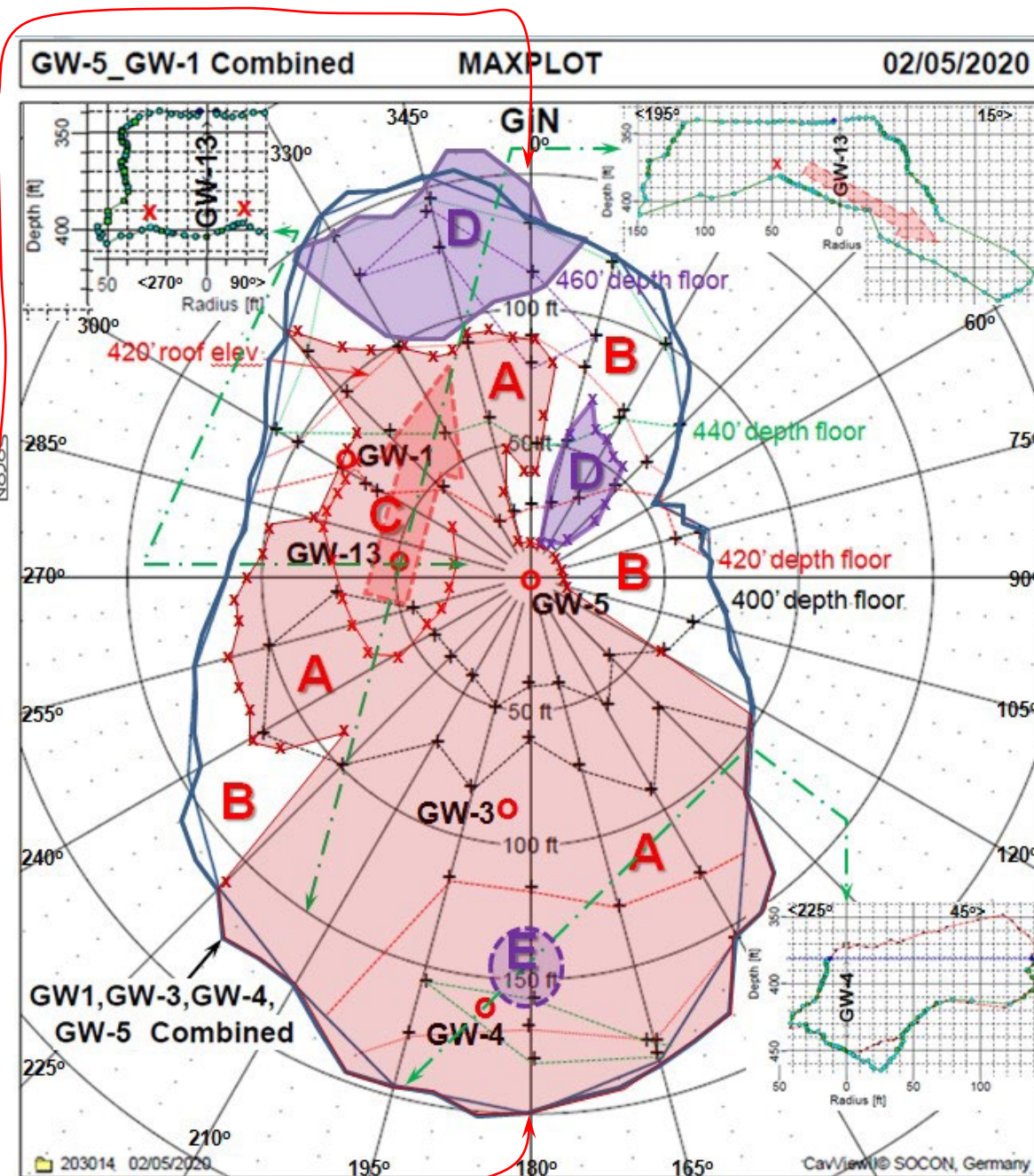
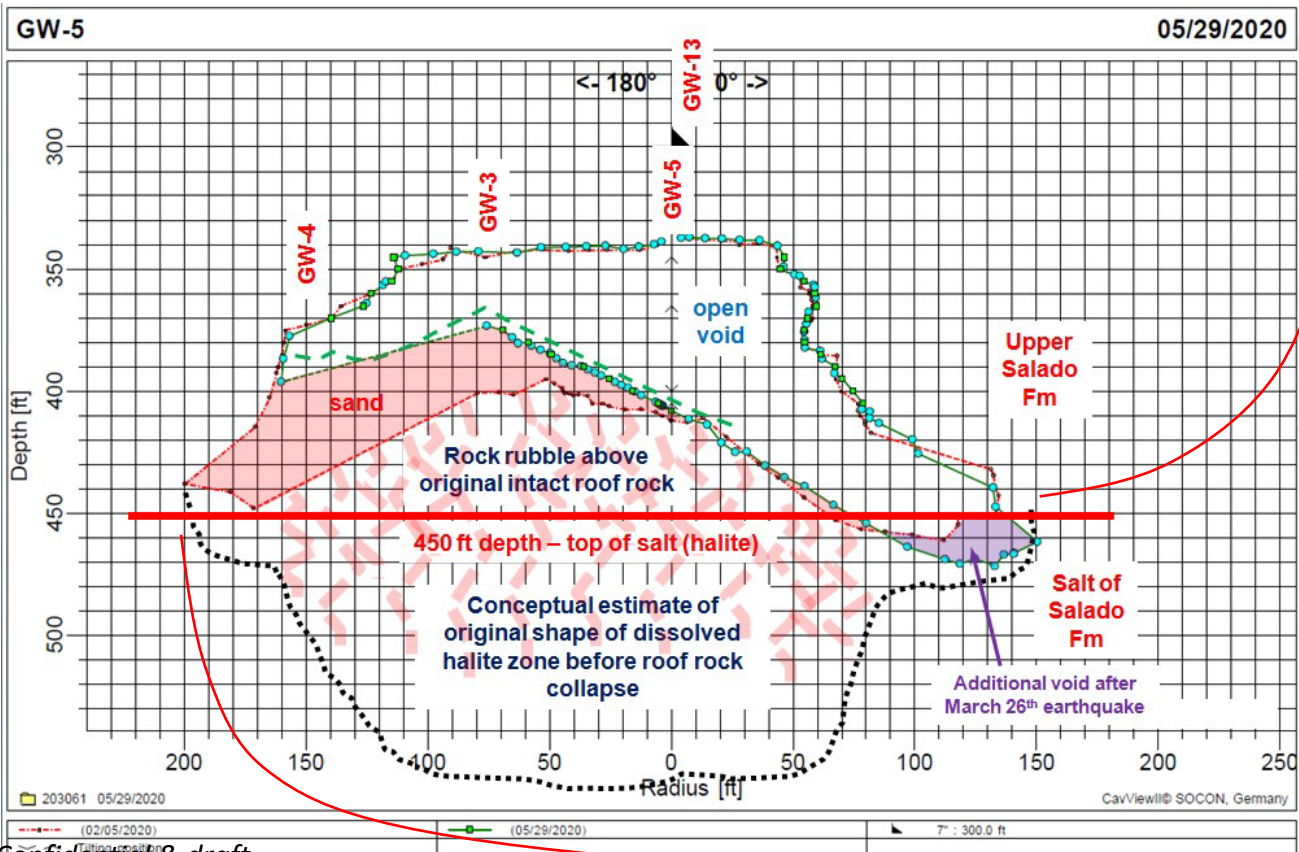


Enhanced onsite micro-seismic network, operational in 2019

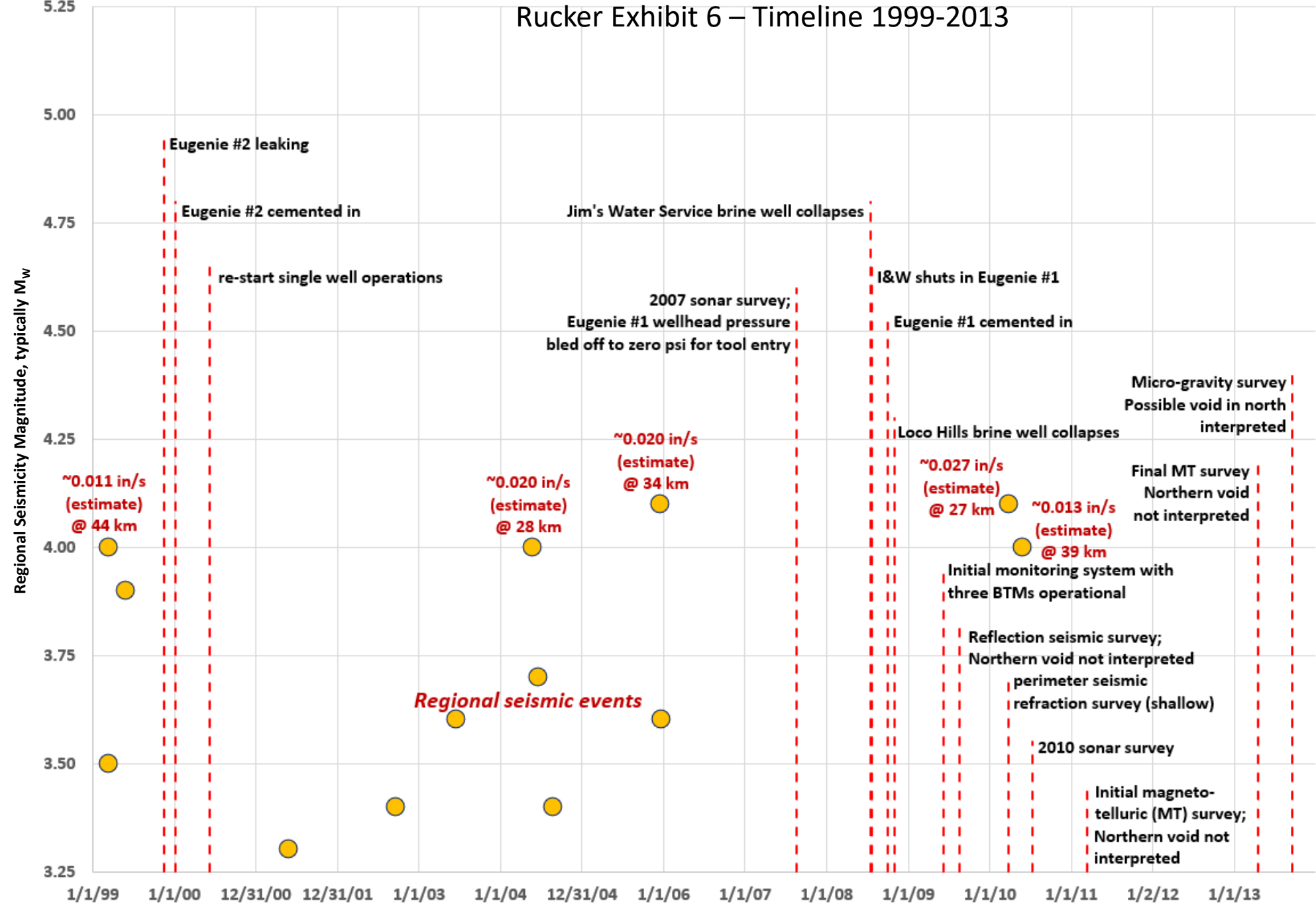
Rucker Exhibit 5 – Likely Void Floor Roof Rock Rubble Response to 3/26/2020 Seismic Activity

Analysis is based on comparison of Feb 2020 and May 2020 sonar surveys

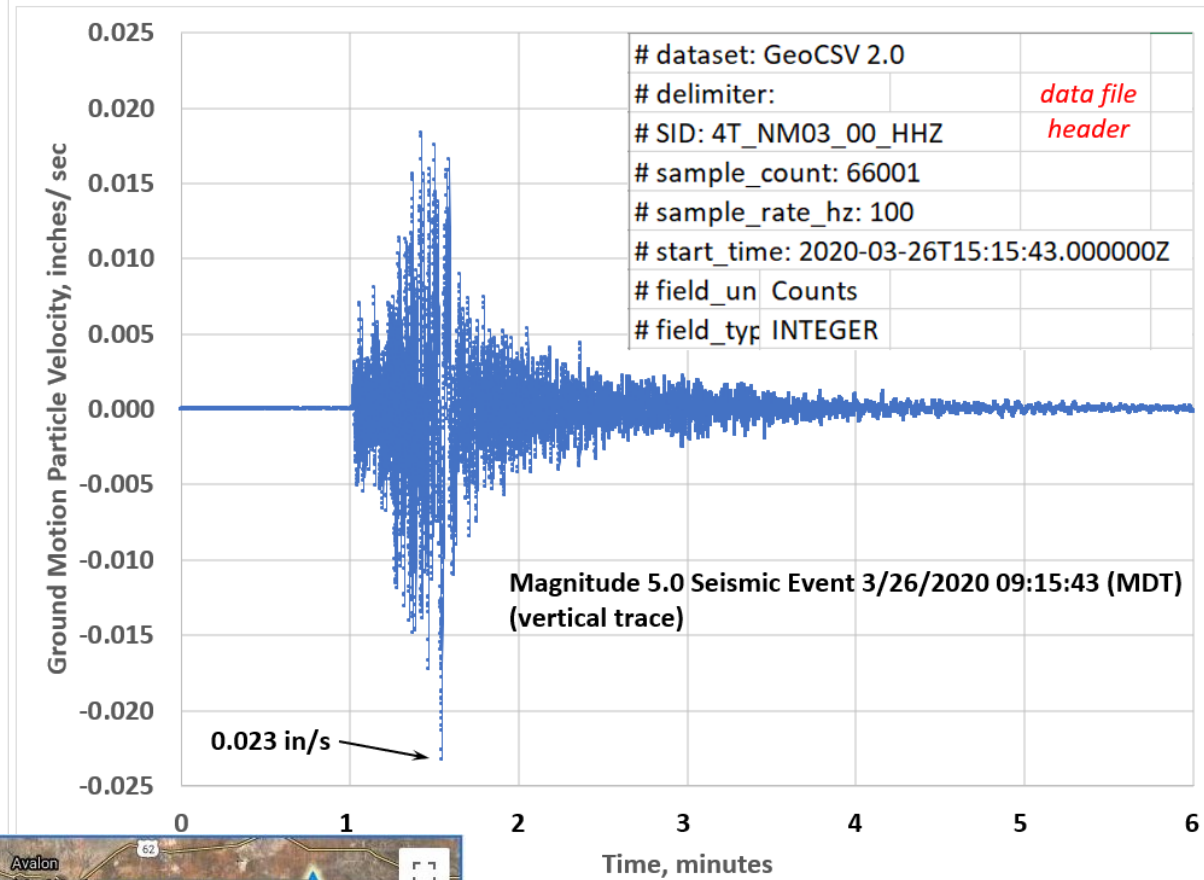
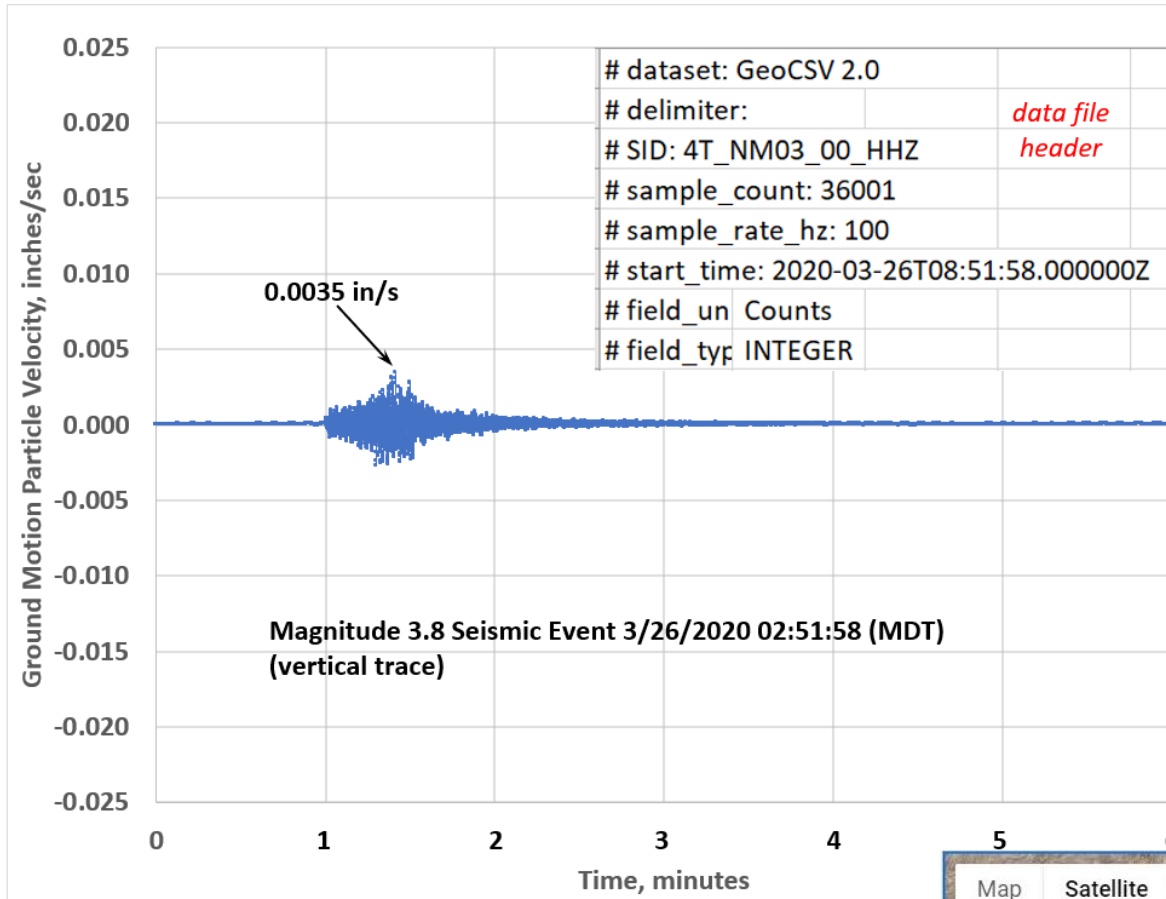
Red shaded area 'A' was the extent of at least several feet of sand accumulation on the void floor (top of rock roof rubble) by late May 2020. Unshaded areas labeled 'B' show the interpreted extent of open void floor which, as of late May 2020, did not have apparent sand accumulation. Sand slide area 'C' was below well GW-13 where sand deployment was focused. As a sand pile developed during sand deployment, the pile would build up until it became unstable and failed by slumping to the north. Interpretable void floor settlement areas labeled 'D' are shaded in purple. Settlement areas are presumed to have resulted from forces acting to compress parts of the loose pile of roof rock debris in response to the March 26th Magnitude 5.0 earthquake. The 'E' settlement area was identified between the mid-January and early February sonar surveys; it was likely not related to seismic activity.



Rucker Exhibit 6 – Timeline 1999-2013



Rucker Exhibit 7 – Calibrated Ground Motion Measurements in the Area



Station 4T.NM03 uses a Trillium seismometer.

That instrument's manual is available online to document scaling for ground motion data, which is in an integer count format in the downloadable files. The 3/26/2020 Mag 5.0 event epicenter was about 93 km from that station. The event was about 75 km from the Brine Cavity. NM03 provides a reasonable and scalable data comparison for the site since a seismic monitoring station is lacking in Carlsbad.

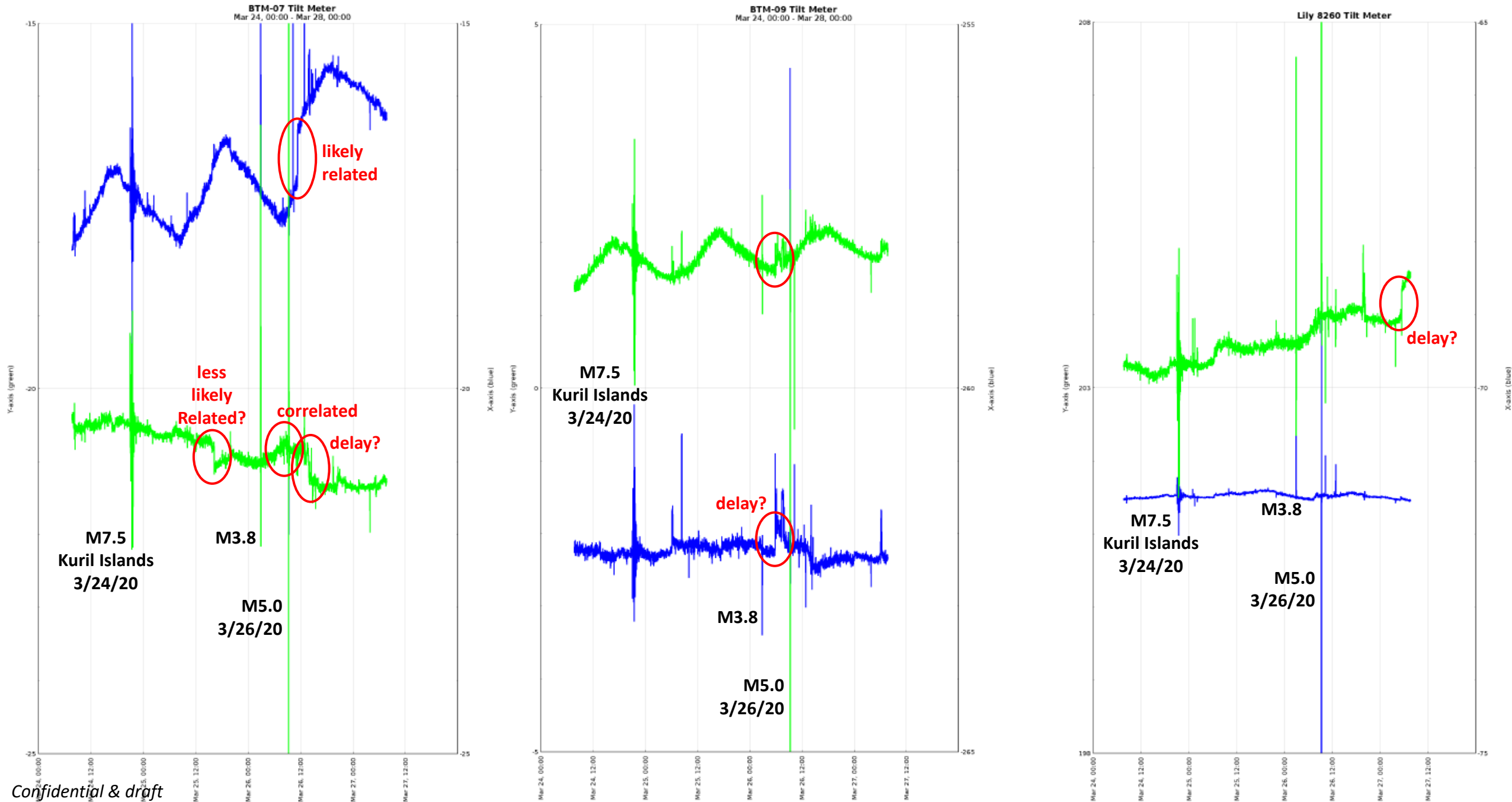
Seismic event duration increases with magnitude.

During the magnitude 5.0 event, seismic signal significantly higher than 'background noise' persists for several minutes. Similar seismic signal during the magnitude 3.8 event persists for only one to two minutes.

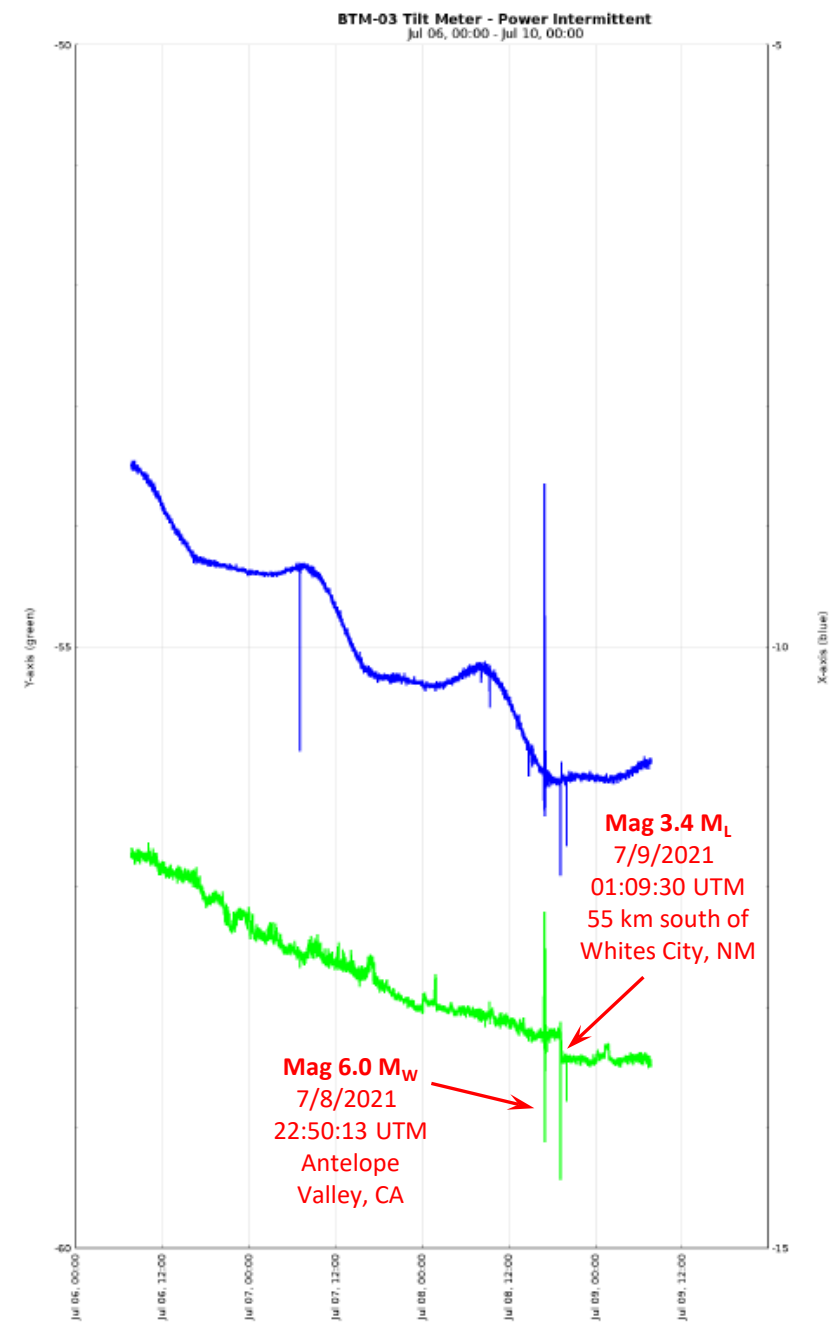
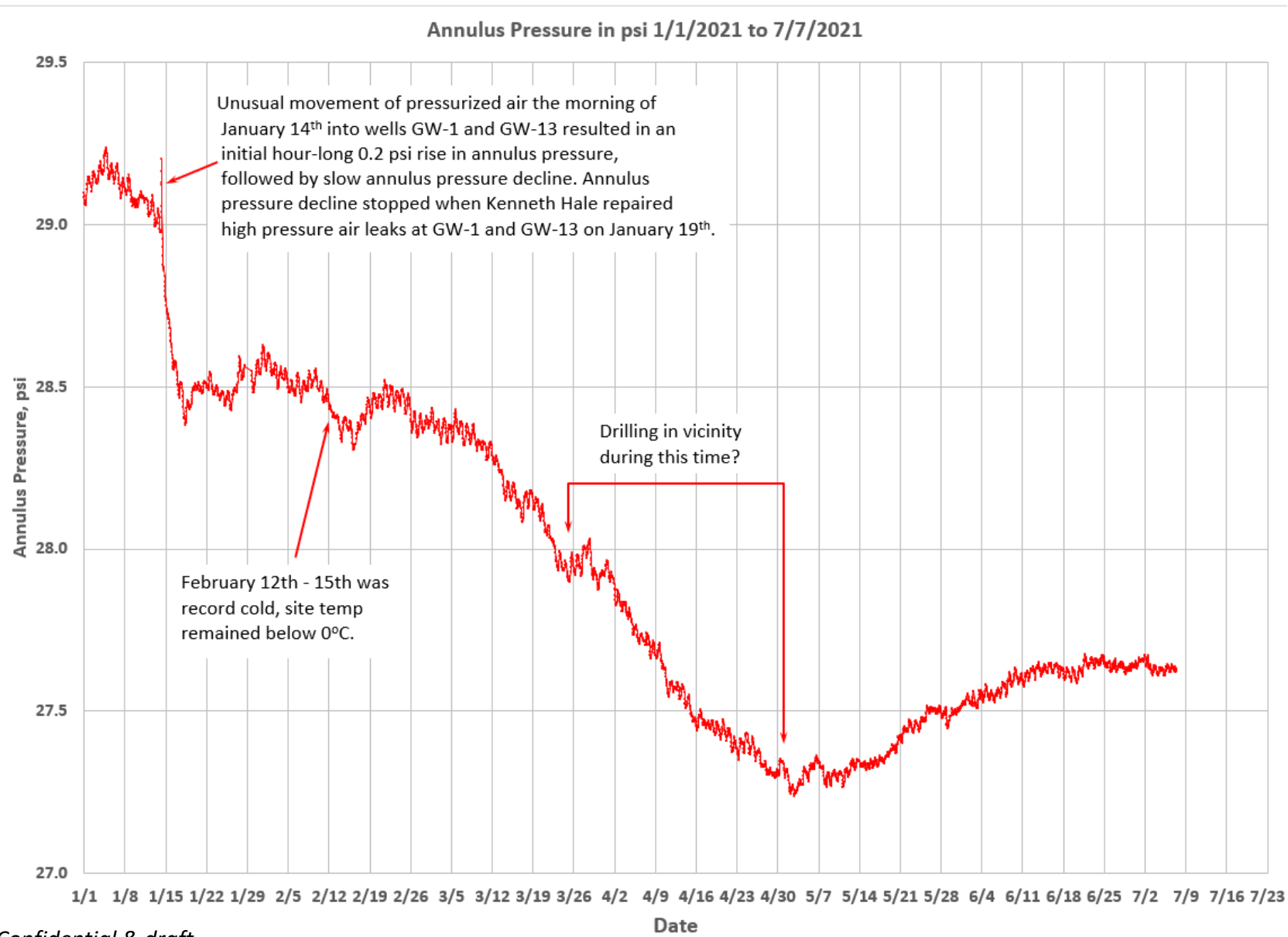
Micro-seismic events located and quantified by the onsite system are within a range of magnitude zero (0) to less than -2, and are typically in a range of magnitude -1 to -2. Durations of these micro events are typically a few tenths of a second.

Confidential & draft

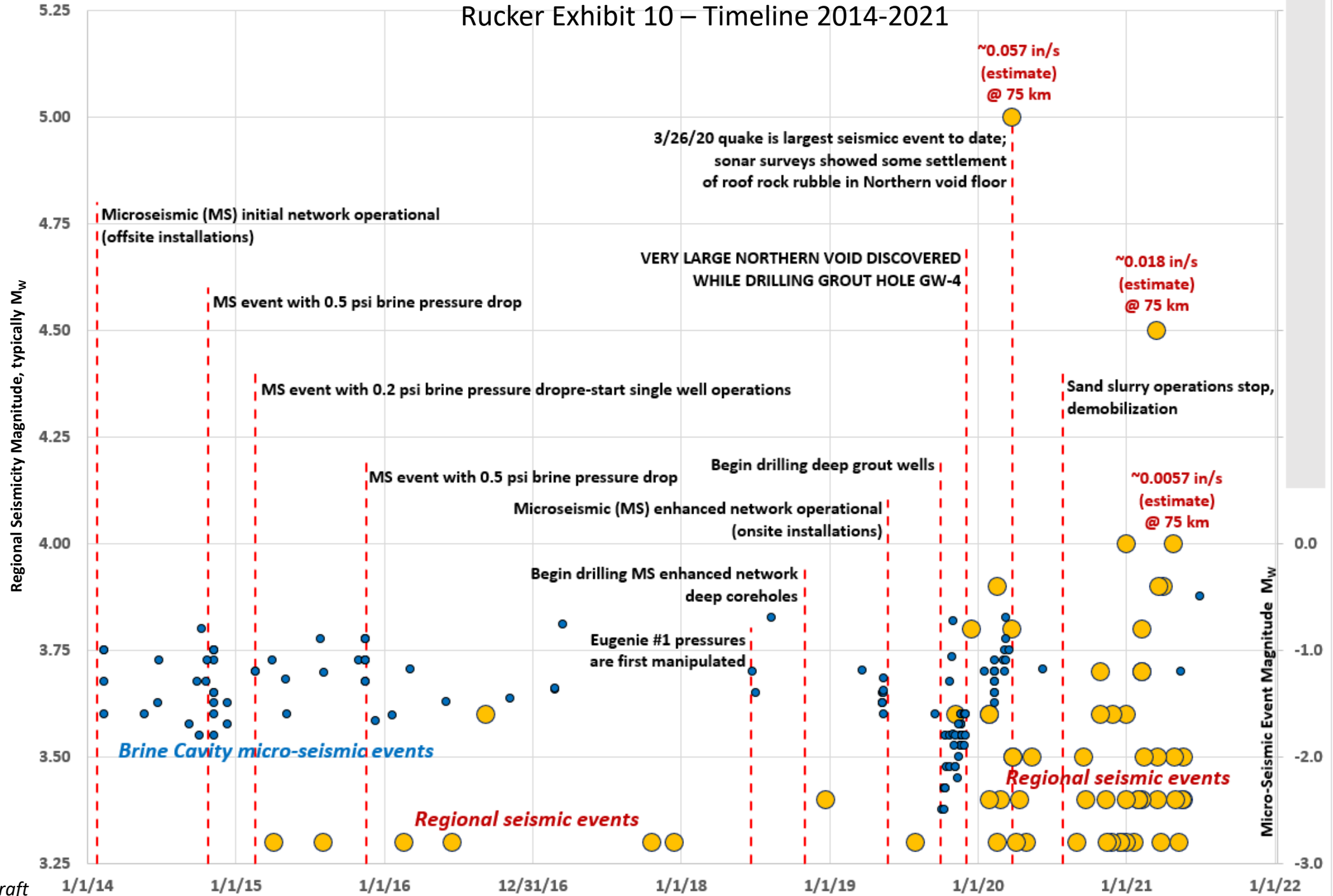
Rucker Exhibit 8 – Borehole Tiltmeter Instrumentation Response to 3/26/2020 Seismic Activity



Rucker Exhibit 9 – Other Example Recent Instrument Responses



Rucker Exhibit 10 – Timeline 2014-2021



Rucker Exhibit 11 – Ground Motion Estimation and Scaling

from Monitoring Memorandum No. 9, May 5, 2020:

General estimates of ground motion based on earthquake magnitude

Attenuation relationships*		Central US*	Western US*
Distance from epicenter	km	75	75
Moment Magnitude	M_L	5.0	5.0
Peak horizontal ground velocity	cm/sec	0.24	0.14
Peak horizontal ground velocity	inches/sec	0.093	0.057
Peak horizontal ground acceleration	cm/sec ²	19.6	10.2
Peak horizontal ground acceleration	g	0.020	0.010

*summarized by Hasegawa, H.S., Basham, P.W. and Berry, M.J., 1981. "Attenuation relations for strong seismic ground motion in Canada," BSSA 71(6), 1943-1962.

Where the Western US equation (Excel format) is:

Peak Ground Velocity (PGV), cm/sec = $0.0004 * \text{EXP}(2.3 * M) * R^{-1.3}$
 where M is moment magnitude, and
 R is distance from epicenter in km

Distance Km	Moment Magnitude	Estimated PGV inches/sec	Measured PGV (vert) inches/sec
Station T4.NM03 Estimated & Measured			
92.6	5.0	0.043	0.023 see Exhibit C
92.6	3.8	0.0027	0.0035 see Exhibit C
Waste Fluid Injection Distances (current)			
75.0	5.0	0.057	
75.0	4.0	0.0057	
75.0	3.0	0.00057	
Fracking Distances (future)			
3.3	3.0	0.033	
3.3	2.0	0.0033	
3.3	1.0	0.00033	
3.3	0.0	0.000033	

Confidential & draft

@ M = 2.0, 3.3 km, modeled PGV $\sim 7 * 10^{-5}$ m/s = ~ 0.0028 in/sec

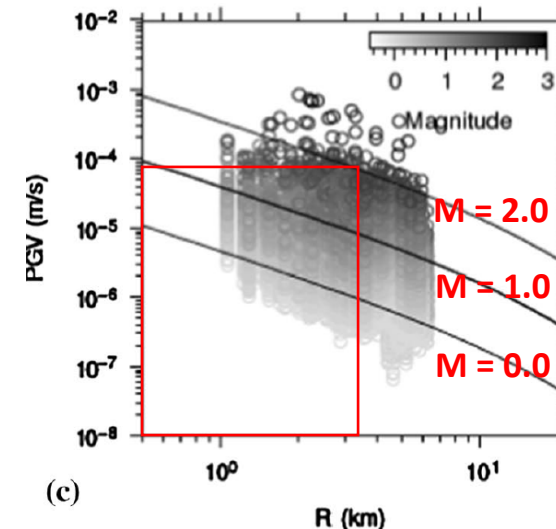


Fig. 2 **a** Magnitude distribution for the catalogue used to infer the reference model (MODREF). **b** Sample distribution of the focal mechanism angles (strike, dip and rake) for the same catalogue. **c** PGVs as function of distance used to infer MODREF. Circles are color coded according to the magnitude of the earthquake. The black lines correspond to the inferred GMPE computed for magnitude values M 0, 1 and 2. **d** Normality plot for the

Acta Geophysica (2020) 68:723–735
<https://doi.org/10.1007/s11600-020-00441-0>

Source:

RESEARCH ARTICLE - ANTHROPOGENIC HAZARD



Using ground motion prediction equations to monitor variations in quality factor due to induced seismicity: a feasibility study

Vincenzo Convertito¹ · Raffaella De Matteis² · Roberta Esposito³ · Paolo Capuano³

Received: 21 January 2020 / Accepted: 3 May 2020 / Published online: 17 May 2020
 © The Author(s) 2020

Abstract

Sub-surface operations for energy production such as gas storage, fluid reinjection or hydraulic fracking may modify the physical properties of the rocks, in particular the seismic velocity and the anelastic attenuation. The aim of the present study is to investigate, through a synthetic test, the possibility of using empirical ground-motion prediction equations (GMPEs) to observe the variations in the reservoir. In the synthetic test, we reproduce the expected seismic activity (in terms of rate, focal mechanisms, stress drop and the b value of the Gutenberg-Richter) and the variation of medium properties in terms of the quality factor Q induced by a fluid injection experiment. In practice, peak-ground velocity data of the simulated earthquakes during the field operations are used to update the coefficients of a reference GMPE in order to test whether the coefficients are able to capture the medium properties variation. The results of the test show that the coefficients of the GMPE vary during the simulated field operations revealing their sensitivity to the variation of the anelastic attenuation. The proposed approach is suggested as a promising tool that, if confirmed by real data analysis, could be used for monitoring and interpreting induced seismicity in addition to more conventional techniques.